Global Gas Transfer Velocity Fields Derived from TOPEX and Jason-1 Normalized Backscatter

Nelson M. Frew, David M. Glover and Scott J. McCue
Woods Hole Oceanographic Institution, Woods Hole, MA 02543

PROJECT OVERVIEW

Global and regional estimates of ocean-atmosphere gas fluxes are limited by the uncertainties in current wind speed - gas transfer velocity parameterizations [Boutin *et al.*, 2002]. These model functions assume wind to be the sole factor controlling gas transfer. The validity of these relationships is hotly debated since they are poorly constrained by field data and generally produce widely varying global oceanic flux estimates (*e.g.* in the case of CO_2, from 1.2 to 2.7 GtC/yr). However, many other factors, including boundary layer stability, variable fetch and surfactant films strongly affect sea surface roughness and thus, the near-surface turbulence that promotes gas transfer.

The goal of this project is to develop an algorithm for estimating regional and global air-sea gas exchange rates using the dual-frequency TOPEX and Jason-1 altimeters. The approach is based on parameterization of the gas transfer velocity (k) using normalized radar backscatter as a direct measure of sea surface roughness due to small-scale waves. The mean square surface slope for waves in the gravity-capillary region of the slope spectrum is a robust predictor of transfer velocity and can be estimated from nadir-looking microwave altimeters using a geometric optics specular scattering model [Jackson *et al.*, 1992]. Mean square slope is inversely related to the normalized backscatter. The differential scattering of the Ku-band and C-band pulses allows us to isolate the contribution of small-scale waves to mean square slope and gas transfer. The differenced mean square slope for the nominal wavenumber range 40-100 rad/m is estimated as:

$$\langle s_n^2 \rangle = \rho_n'^{Ku}/\sigma_o^{Ku} - \rho_n'^{C}/(\sigma_o^{C} + \alpha)$$

where ρ'^{Ku}_n and ρ'^{C}_n are effective nadir reflectivities, σ_o^{Ku} and σ_o^{C} are normalized Ku-band and C-band backscatter coefficients and α is an *ad hoc* adjustment to σ_o^{C} [Chapron *et al.*, 1995]. The parameters for estimating the differenced mean square slope are optimized using *in situ* optical slope measurements to give $\rho'^{Ku}_n = 0.40$, $\rho'^{C}_n = 0.51$ and $\alpha = 1.36$. An empirical relationship between gas transfer velocity and differenced mean square slope is derived from field and laboratory measurements of gas flux and optical slope:

$$k_{Sc(T)} = \left(\frac{Sc(T)}{660}\right)^{-0.5} (C_0 + C_1(\langle s_n^2 \rangle)^2)$$

where k_T is the gas transfer velocity in units of cm h^{-1} at sea surface temperature T, Sc is the Schmidt number, C_0 = 0.697 and C_1 = 8.02E+5.

The algorithm is used to construct monthly global maps of gas transfer velocity and to estimate seasonal transfer velocity variations.

ACKNOWLEDGMENT

This research has been supported by the National Aeronautics and Space Administration through Grant NAGW-2431 (JPL Contract 961425).

SLOPE VS. U_{10} PARAMETERIZATIONS

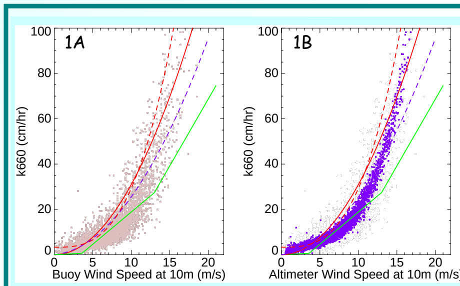

Figure 1. TOPEX-derived k_{660} vs. buoy (1A) and altimeter (1B) wind speed at 10 m height.

Data set consists of ~4350 collocated buoy and altimeter observations [Gommenginger *et al.*, 2002]. Four idealized gas k-U_{10} relationships are also shown: Wanninkhof [1992] quadratic relation for short term or steady winds (solid red); McGillis *et al.* [2001] cubic relation derived from CO_2 flux observations (dashed red); Nightingale *et al.* [2000] quadratic relation derived from dual tracer release experiments (dashed blue); Liss and Merlivat [1986] synthesis from wave tank and lake observations (solid green).

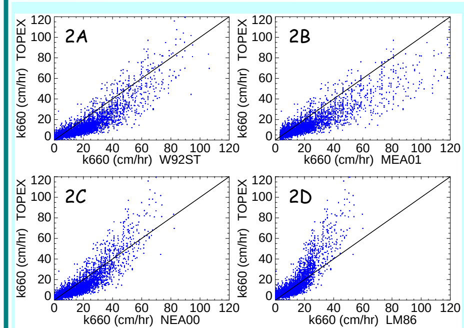

Figure 2. Comparison of altimeter-derived k_{660} estimates with those computed from four commonly used gas transfer velocity-wind speed relationships: Wanninkhof, 1992 (2A); McGillis *et al.*, 2001 (2B), Nightingale *et al.*, 2000 (2C); and Liss-Merlivat, 1986 (2D).

TOPEX MULTI-YEAR TIME SERIES

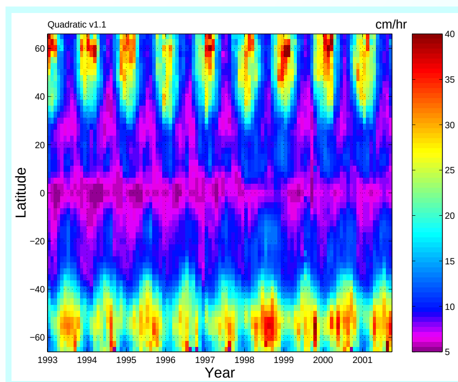

Figure 3. Time-series of TOPEX-derived monthly zonal average k_{660} for the period January, 1993-September, 2001 (cycles 11-330) computed on a 2.5° x 2.5° grid. Values in units of cm h^{-1} for Schmidt number Sc = 660 (Sc = 660 for CO_2 at 20°C in seawater).

Data, individual monthly images and time-series animation available at: http://remotesensing.whoi.edu/~david/ktrans.

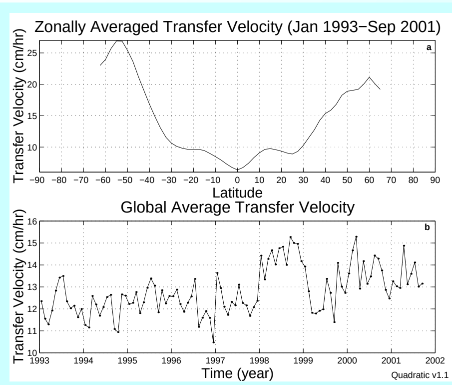

Figure 4. 1993-2001 global climatology from the time series: (a) average zonal transfer velocities and (b) global monthly average transfer velocities.

Features apparent in the time series include:

- hemispheric asymmetry - highest avgs. at 50-60 S;
- N mid-latitude summer lows - not matched in S;
- global average k_{660}= 13 cm h^{-1} vs. 17 cm h^{-1} for Wanninkhof *et al.*, 2002;

An apparent upward trend in transfer velocity begins with a pulse in early '98, followed by a return to earlier average levels (coincident with switch to B-side) and then trending upward again.

Global Gas Transfer Velocity Fields Derived from TOPEX and Jason-1 Normalized Backscatter

Nelson M. Frew, David M. Glover and Scott J. McCue
Woods Hole Oceanographic Institution, Woods Hole, MA 02543

EARLY JASON-1 VS. TOPEX RESULTS

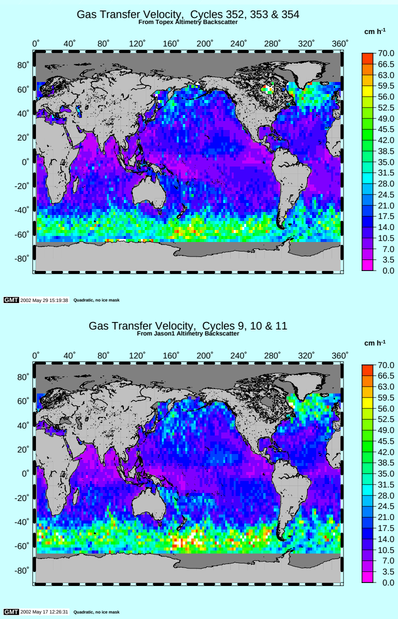

Figure 5. Monthly average global transfer velocity fields for TOPEX Cycles 352, 353 and 354 (upper) and Jason-1 Cycles 009, 010 and 011 (lower) adjusted to 20°C. No ice mask has been applied.

General patterns observed with both altimeters are similar, but the Jason-1 product appears generally 'hotter', especially in higher latitude regions where k_{660} values are highest.

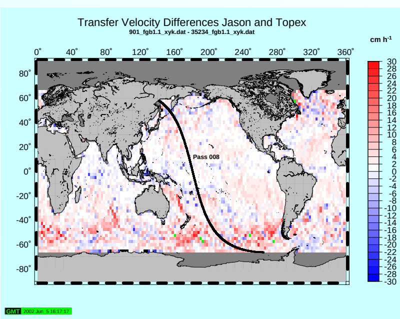

Figure 6. The Jason-TOPEX difference map (Δk_{660}) for the cycles in Figure 5. The heavy black line represents an over-water pass (008) of the tandem orbit.

The difference map shows:
•elevated Δk_{660} over large areas of southern ocean and east of Australia;
•small negative Δk_{660} in the equatorial region (0-5°N).

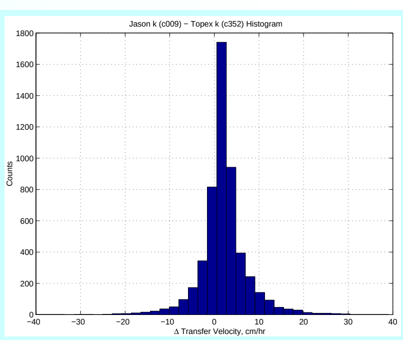

Figure 7. Histogram of Δk_{660} (Jason-TOPEX) global field from Fig. 6.

There is clearly a positive bias in the Jason estimates relative to TOPEX. The global mean Δk_{660} is +2.1 cm h^{-1}, with most of the deviations falling within ±20 cm h^{-1}.

ALONG-TRACK Ku and C-BAND BIASES

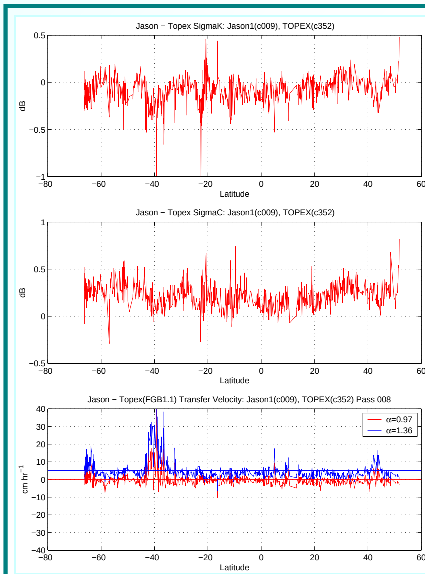

Figure 8. Along-track Ku- and C-band differences (Jason-TOPEX) and Δk_{660} for trans-Pacific pass 008 (Cycles 009 and 352).

Comparison of σ_0^{Ku} and σ_0^{C} between Jason and TOPEX in this over-water pass shows significant bias in both bands. The σ_0^{Ku} shows a negative bias of ~ 0.08 dB, while a positive bias of ~0.22 dB is observed for σ_0^{C}. These result in a mean along-track k_{660} difference of ~5.1 cm h^{-1}, with perturbations as large as 30+ cm h^{-1}. The along-track average difference can be reduced to zero with an ~30% reduction in the *ad hoc* C-band correction (α).

Globally, this correction would be much smaller (of order 10%) since the global Jason-TOPEX Δk_{660} is much lower than for the individual pass illustrated here. These results are very preliminary and may be influenced by processing difficulties in our Jason-1 IGDR and TOPEX GPC data ingests. However, they strongly suggest that a closer examination of variability in σ_0^{Ku} - σ_0^{C} relations will be required to achieve internal consistency in this and other dual frequency applications [Quartly, 1999].

SUMMARY

•The slope parameterization produces transfer velocities similar to those from commonly used wind-speed parameterizations; however, the global climatology yields an average global transfer velocity ~30% lower than that predicted by the Wanninkhof, 1992 wind speed model.

•Climatology also suggests trend toward higher average zonal and global transfer velocities beginning in early 1998;

•First look at Jason-1 transfer velocity fields show slightly higher global averages (~ 2 cm hr^{-1}) relative to TOPEX and significantly higher discrepancies (~ 20 cm hr^{-1}) at high latitudes (*e.g.* Southern Ocean);

•Comparison of along-track Ku- and C-band σ_0 suggests that the discrepancies are due to significant offsets between TOPEX and Jason-1 in both bands.

REFERENCES CITED

Boutin *et al.* [2002]. *Geophys. Res. Lett.*, **29**, 23-1—23-4.
Chapron *et al.* [1995]. In: *Air-Water Gas Transfer*, Jaehne & Monahan (eds), AEON Verlag, Hanau, 869-878.
Gommenginger *et al.* [2002]. *IEEE Trans. Geosci. Remote Sens.*, **40**, 251-260.
Jackson *et al.* [1992]. *J. Geophys. Res.*, **97**, 11411-11427.
Liss and Merlivat [1986]. In: *The Role of Air-Sea Exchange in Geochemical Cycling*, P. Buat-Menard (ed), Reidel, Hingham, MA, 113-127.
McGillis *et al.* [2001]. *J. Geophys. Res.*, **106**, 16729-16745.
Nightingale *et al.* [2000]. *Global Biogeochem. Cycles*, **14**, 373-387.
Quartly, G. [1999] Joint TOPEX/Poseidon-Jason-1 SWT Mtg., St. Raphael, FR.
Wanninkhof [1992]. *J. Geophys. Res.*, **97**, 7373-7382.
Wanninkhof *et al.* [2002]. In: *Gas Transfer at Water Surfaces*, M. Donelan *et al.* (eds), AGU Geophysical Monograph **127**, 351-356.